Materials and Design 55 (2014) 542–550

Contents lists available at ScienceDirect

Materials and Design

journal homepage: www.elsevier.com/locate/matdes

Out-of-plane constraint effect on local fracture resistance of a dissimilar metal welded joint

J. Yang, G.Z. Wang *, F.Z. Xuan, S.T. Tu, C.J. Liu

Key Laboratory of Pressure Systems and Safety, Ministry of Education, East China University of Science and Technology, Shanghai 200237, China

ARTICLE INFO

Article history:
Received 7 August 2013
Accepted 12 October 2013
Available online 23 October 2013

Keywords:
Out-of-plane constraint
Local fracture resistance
Dissimilar metal welded joint
Fracture mechanism
Safety design

ABSTRACT

An experimental investigation on effect and mechanism of out-of-plane constraint induced by specimen thickness on local fracture resistance of two cracks (A508 heat-affected-zone (HAZ) crack and A508/Alloy52Mb interface crack) located at the weakest region in an Alloy52M dissimilar metal welded joint (DMWJ) between A508 ferritic steel and 316L stainless steel in nuclear power plants has been carried out. The results show with increasing out-of-plane constraint (specimen thickness), the fracture mechanism of the two cracks changes from ductile fracture through mixed ductile and brittle fracture to brittle fracture, and the corresponding crack growth resistance decreases. The crack growth path in the specimens with different out-of-plane constraints deviates to low-strength material side, and is mainly controlled by local strength mismatch. For accurate and reliable safety design and failure assessment of the DMWJ structures, it needs to consider the constraint effect on local fracture resistance. The new safety design and failure assessment methods incorporating both in-plane and out-of-plane constraint effects need to be developed for the DMWJ structures.

1. Introduction

It is well known that the constraint of cracked structures includes in-plane constraint and out-of-plane constraint. The in-plane constraint is directly influenced by specimen dimension in the direction of growing crack, i.e. the length of the uncracked ligament for straight through cracks, whilst the out-of-plane constraint is affected by the specimen dimension parallel to the crack front, i.e. the specimen thickness. For a given in-plane configuration, the plane strain state describes the highest out-of-plane constraint, whereas the plane stress state generates the lower limit. In a three-dimensional cracked specimen, the out-of-plane constraint lies between the two limit cases [1]. In the standard fracture toughness tests of deep crack specimens in elastic–plastic fracture mechanics framework, such as in ASTM: E1820 and British standard [2], the specimen thickness B is usually recommended to be half of the width W of specimen. Such restriction is mainly to ensure a plane strain condition in the crack front; thereby the plane strain toughness value (that is the lower limit of material toughness) can be obtained. The use of such bounding data in plant assessments is obviously conservative. As constraint can significantly alter the material's fracture behavior and toughness, it is important to develop a clear understanding of constraint effect on the fracture behavior of materials to increase the accuracy of structural integrity assessment.

The effects of in-plane and out-of-plane constraints on fracture resistance of materials have been studied for a long time. The work of Irwin et al. [3] showed that the specimen thickness has considerable effect on the value of apparent toughness. The apparent toughness decreases dramatically with thickness until a plateau value of the plane strain fracture toughness is reached. The study of Garwood [4] showed that the experimental J–R curves obtained from specimens with different geometries and loading modes were different, and the J-integral resistance curves were considerably affected by constraint. Hancock et al. [5] correlated the geometry dependence of crack tip constraint and fracture toughness by testing a number of cracked specimens. Thesis et al. [6] studied the effect of crack depth on the fracture toughness of reactor pressure vessel steel. Joyce et al. [8,9] investigated the effect of crack depth and loading mode on the J–R curve behavior and fracture toughness of a high-strength steel HY80, etc.

Furthermore, a lot of fracture constraint parameters and theories, such as K–T [10], J–Q [11,12], J–A_2 [13], T_Z [14–16], φ [17,18] and A_p [19,20], have been developed to characterize and analyze the constraint effect. The T-stress is an elastic parameter for characterizing crack-tip constraint, and represents the tensile stress acting parallel to the crack plane [10]. The parameter Q is a constraint parameter quantifying the deviation of opening stress in a non-standard specimen from a standard specimen under elastic–plastic condition, and can effectively describe the constraint effect on the crack-tip field for different geometries under a variety of deformation levels [11,12]. The constraint parameter A_2 is used to relate the first term to the second and third terms of the

* Corresponding author. Tel.: +86 021 64252681; fax: +86 021 64253513.
E-mail address: gzwang@ecust.edu.cn (G.Z. Wang).

0261-3069/$ - see front matter © 2013 Elsevier Ltd. All rights reserved.
http://dx.doi.org/10.1016/j.matdes.2013.10.034

asymptotic stress distribution in an elastic–plastic cracked body [13]. The T_z factor introduced by Guo [14–16] is a parameter to characterize the out-of-plane constraint effect. Variation of these parameters usually has a marked effect on the size of the plastic region ahead of the crack and on the near tip stress distribution. In order to quantify both the in-plane and out-of-plane constraints, Mostafavi et al. [17,18] defined a new constraint parameter φ which quantified constraint by the areas of the plastic zone at the onset of fracture. Yang et al. [19,20] defined a parameter A_p to quantify the constraint by the areas surrounded by the crack-tip equivalent plastic strain (ε_p) isolines for materials with high toughness.

However, all studies mentioned above were mainly for homogeneous materials. The effects of in-plane or out-of-plane constraint on local fracture resistance of highly heterogeneous structures, such as dissimilar metal welded joint (DMWJ), have not been systemically investigated. The DMWJ has been widely used in primary water systems of pressurized water reactors (PWRs) in nuclear power plants (NPPs). But it is vulnerable component of nuclear structures due to the highly heterogeneous of microstructure, mechanical, thermal and fracture properties and some defects produced during manufacture. Different types of defects within DMWJs have been found in the NPPs of many countries [21,22], and serious leakage events on such DMWJs have also been reported [23,24]. Thus, for the DMWJ's safe service, it is critical and essential to develop an accurate safety design and assessment procedure of structural integrity. For doing this, the fracture behaviors of DMWJs under different constraint conditions should be investigated.

Wang et al. [25,26] have studied the local J-resistance curves and fracture mechanism of 13 cracks located at different positions (as shown in Fig. 1) of an Alloy52M DMWJ between A508 ferritic steel and 316L stainless steel (SS). Their results show that the crack 2 at A508 HAZ and the crack 3 at A508/52Mb interface have the lowest J-resistance curves and are the weakest zones for failure in the DMWJ. The effects of in-plane constraint induced by crack depth on local fracture resistance of the cracks 2 and 3 in the DMWJ have been experimentally investigated by authors [27]. In this paper, a further experimental investigation on the effect and mechanism of out-of-plane constraint induced by specimen thickness on local fracture resistance was carried out.

2. Experimental procedures

2.1. Materials and fabrication of the DMWJ

In this study, a real Alloy52M DMWJ between A508 ferritic steel and 316L stainless steel (SS) which is used for connecting the safe end to pipe-nozzle of the reactor pressure vessel in nuclear power plants (NPPs) was used, and it is the same as that used in the previous studies [25–28]. The pipe-nozzle material is ferritic low-alloy steel (A508), and the safe end pipe material is austenitic stainless steel (316L). The weld was manufactured by applying a buttering technique and the buttering material (Alloy52Mb) as well as weld material (Alloy52Mw) is the same nickel-base alloy, but their fabrication procedures were different. The full scale mock up of the DMWJ was detailed in Refs. [25,26,28], and the four materials composed of the DMWJ joint are shown in Fig. 1. The chemical compositions of the four materials are listed in Table 1 [25,26,28].

2.2. Specimen geometry

The single-edge notched bending (SENB) specimens were machined from the Alloy52M DMWJ for measuring the local fracture resistance and observing fracture mechanism. The two weakest positions (the crack 2 and crack 3 in Fig. 1) with the lowest fracture-resistance curves [25,26] were selected. The crack 2 is located in A508 HAZ with a 1.5 mm distance from A508/52Mb interface, and the crack 3 is located in A508/52Mb interface. The specimen width W is 14.4 mm, the crack depth a is 7.2 mm ($a/W = 0.5$), and the loading span S is 57.6 mm ($S = 4W$). To investigate the fracture mechanism and fracture resistance under different out-of-plane constraints, four specimen thicknesses denoted as $B = 6$, 9, 15 and 18 mm (the SENB specimen with $B = 12$ mm has been studied in the Ref. [26]) were chosen. The geometry and loading configuration of the typical crack 2 specimen ($W = 14.4$ mm, $B = 12$ mm and $a/W = 0.5$) are illustrated in Fig. 2. The specimens were not side-grooved, an initial notch with a length of 5.7 mm was prepared by electro-discharge machining, and then a fatigue pre-crack with a length of 1.5 mm was made in the specimens.

2.3. Experiments and observations

The fracture tests of the SENB specimens were performed by an Instron screw-driven machine at room temperature. The quasi-static loading was conducted by displacement controlled mode at a cross-head speed of 0.5 mm/min, and the load-load line displacement curves were automatically recorded by a computer aided control system of the testing machine. The single specimen method and the normalization technique conforming the ASTM: E1820 were used to obtain the J-resistance curve for each specimen, and it has been described in the previous study [26].

After testing, the tested specimens were sectioned at the mid-plane to observe the crack growth path and the fracture surface, as shown in Fig. 3. One of the cut pieces was polished and etched to reveal crack growth path, and then observed by a scanning electron microscope (SEM). The A508 ferritic steel was etched with a solution of 4% nitric acid in alcohol, while the Alloy52Mb was etched with a solution of 16 g$FeCl_3$ + 80 mlHCl + 2 mlHNO_3 + 11 mlH_2O. Another piece was broken, and the final crack growth length was measured and the fracture surfaces were also observed with the SEM to understand the fracture mechanism.

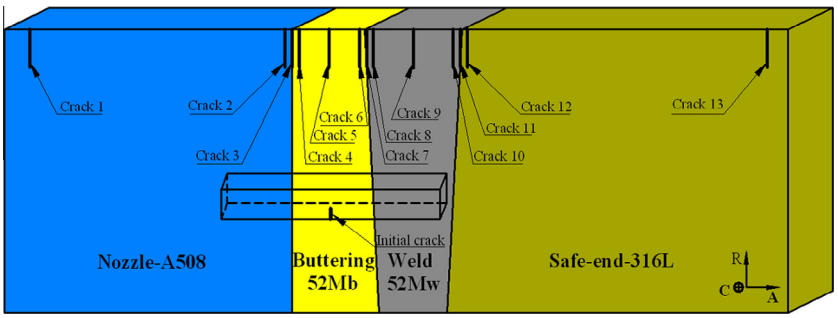

Fig. 1. The four materials composed of the DMWJ and initial crack positions [25,26,28].